Electronic Supplementary Material (ESI) for Journal of Materials Chemistry A.

Synthesis of Cu-Ir Nanocages with Enhanced Electrocatalytic Activity for the Oxygen Evolution Reaction

Chao Wang,[a] Yongming Sui,*[a] Guanjun Xiao,[a] Xinyi Yang,[a] Yingjin Wei,[b] Guangtian Zou,[a] and Bo Zou*[a]

[a] *State Key Laboratory of Superhard Materials, Jilin University, Changchun 130012, china. E-mail: zoubo@jlu.edu.cn; suiym@jlu.edu.cn*

[b] *Key Laboratory of Physics and Technology for Advanced Batteries (Ministry of Education), College of Physics, Jilin University, Changchun 130012, China.*

1. Chemicals and Materials

Iridium (III) chloride hydrate ($IrCl_3$ 99.9%) and oleylamine (OLA $\geq$ 70%) were obtained from Alfa Aesar. Copper (II) acetylacetonate ($Cu(acac)_2 \geq$ 99.99%) were purchased from Aldrich. Toluene and methanol were commercially available analytical-grade products. All chemicals were used without further purification in experiments.

2. Synthesis of Cu-Ir hollow porous nanostructures

The $IrCl_3$-OLA solution was prepared in a Schlenk line by dissolving 0.2 mmol of $IrCl_3$ in 1mL of OLA at 120 ^oC for 30 min. In a typical synthesis, 0.2 mmol of $Cu(acac)_2$ and 5 mL of OLA were loaded into a 50 mL three-neck flask equipped with rubber septum in a glove box. Then the flask was sealed and taken out to connect to the Schlenk line equipped with a condenser. The mixture was heated gradually under a nitrogen flow and vigorous magnetic stirring to 270 ^oC and kept at this temperature for 15 min. After that, the temperature was immediately decreased to 250 ^oC and then the pre-made solution of $IrCl_3$-OLA was injected swiftly into the reaction mixture. The reaction mixture was maintained at 250 ^oC for 2 h and then cooled down to room temperature. Finally, the black precipitate from the reaction solution was isolated by centrifugation at a speed of 13000 rpm and washed with toluene and methanol for three times, and then a trait of chloroform and excess amount of acetone were added to be washed for another two times. Finally the products were dissolved in nonpolar solvents to form stable colloidal solutions. Moreover, Cu core Cu-Ir shell core-shell nanoparticles were also synthesized by changing the precursor ratios of $IrCl_3/Cu(acac)_2$ to 1:3 and 2:3, respectively.

3. Synthesis of Ir NDs

Ir NDs were synthesized in organic solvents using a previously reported method from our group.[1] Briefly, 0.33 mmol of $IrCl_3$ and 5 mL of ODA were added into a 50 mL three-necked flask. The mixture was gradually heated to 120 ^oC under a nitrogen flow and vigorous magnetic stirring conditions and kept at this temperature for 30 min to remove trace water and oxygen. Then, the temperature was increased to 290 ^oC at a rate of 10 ^oC/min and maintained at this temperature for 20 min. After that, the reaction mixture was cooled down to room temperature. The black precipitate from the reaction solution was isolated by centrifugation at a speed of 13000 rpm and washed with toluene and methanol for three times and then a trait of chloroform and excess amount of acetone were added to be washed for another two times. Finally, the products were dissolved in nonpolar solvents to form stable colloidal solutions.

4. Characterization

Powder X-ray diffraction (XRD) spectra were recorded on a Shimadzu XRD-6000 X-ray diffractometer operating at 40 KV and 40 mA with Cu kα radiation. Data were collected from 30° to 90° with a sampling interval of 0.02° per step and a scan speed of 4°/min. Samples for transmission electron microscopy (TEM) characterization were suspended in toluene; then several drops of the suspension was added onto a 300-mesh molybdenum grid with carbon support film. TEM and high-resolution TEM (HRTEM) images were acquired with a JEM-2200FS TEM operating at 200 KV. Composition of the specimens was examined using energy-dispersive X-ray (EDX) spectroscopy and scanning transmission electron microscopy mapping (STEM-mapping) attached to the JEM-2200FS. Field-emission scanning electron microscopy (FESEM) images were recorded on a FEI Magellan 400L microscope operating at 18 kV. The ultraviolet-visible infrared (UV-vis) absorption spectra were performed by an optical fiber spectrometer (Ocean Optics, QE65000). Inductively coupled plasma atomic emission spectrometry (ICP-AES) was performed with a PerkinElmer OPTIMA 3300 DV analyzer. X-ray photoelectron spectroscopy (XPS) was investigated by using a VG ESCALAB MKII spectrometer with a Mg KR excitation (1253.6 eV).

5. Measurements of electrocatalytic activities of oxidation evolution reaction

The electrochemical catalytic activity investigation was performed with a CHI 660E electrochemical workstation (Shanghai Chenhua Apparatus, China). The working electrode was a catalyst-coated glassy carbon (GC) electrode (d = 3 mm, geometric area 0.07 cm^2). The Pt wire with a diameter of 1 mm and Hg/$HgSO_4$ (CHI, in saturated K_2SO_4) were used as counter electrode and reference electrode, respectively. To prepare the working electrode, a GC electrode was first polished with an alumina slurries (0.05 μm), and then cleaned by sonication in distilled water for 3 min to remove any alumina residue, and then allowed to dry. For $Cu_{1.1}Ir$, $Cu_{1.4}Ir$, Cu_2Ir and Ir NDs, 10 mg of catalysts were dispersed in 2 mL toluene and sonicated for 3 min. For Ir black, 10 mg of catalysts were dispersed in 2 mL aqueous solution. 2 μL of the catalyst ink was pipetted onto the pre-polished GC electrode surface by a microliter syringe, and the working electrodes were obtained after the solvent was dried naturally, which results in a catalyst loading of 10 μg. 0.05 M H_2SO_4 aqueous solution deoxygenated with purified nitrogen was used as the supporting electrolyte. All potentials reported in this paper were normalized with respect to the reversible hydrogen electrode (RHE). To prepare catalytic active water splitting catalyst, the electrochemical dealloying and oxidation process was performed for these Cu-Ir alloy NPs, Ir NDs and commercial Ir black, respectively, within the potential range from 0 to 1.46 V at a scan rate of 100 mV/s for 20 cycles. The electrocatalytic activity of these catalysts was studied by using linear sweep voltammetry between 1.1 V to 1.56 V with a scan rate of 5 mV/s. Compensation for iR drop was used for catalytic activity measurements. Chronopotentiometry curves were recorded at 0.07 mA, resulting in a current density of 1 mA/cm^2, in 0.05 M H_2SO_4 solution under magnetic stirring at 2000 rpm for 5 h to investigate the stability of these electrocatalysts.

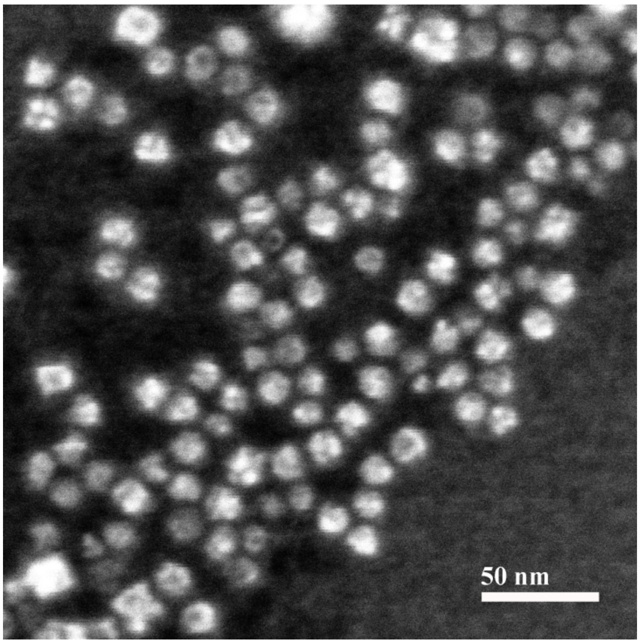

Fig. S1 FESEM image of the as-prepared $Cu_{1.11}Ir$ NCs. Holes on their surfaces could be observed.

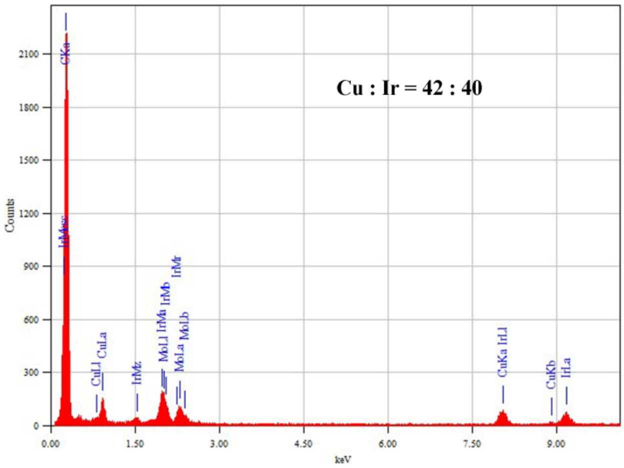

Fig. S2 EDX spectrum of the as-prepared $Cu_{1.11}Ir$ NCs. The atom ratio of Cu to Ir is 42 : 40.

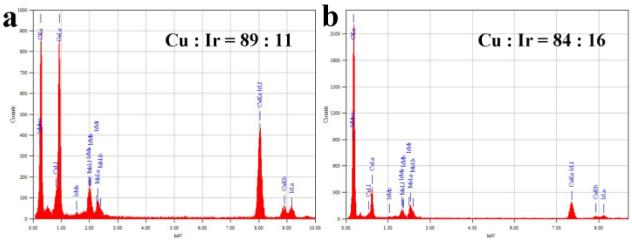

Fig. S3 EDX spectra of the products obtained after the injection of $IrCl_3$-OLA for 5 min (a) and 15 min (b). With the reaction time increasing from 5 to 15 min, the content of Ir in the products increases.

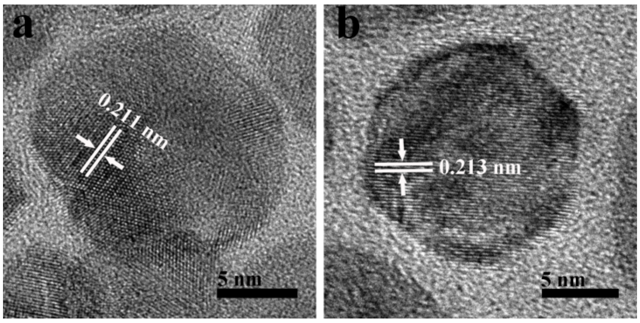

Fig. S4 HRTEM images of the products obtained after the injection of $IrCl_3$-OLA for 5 min (a) and 15 min (b).

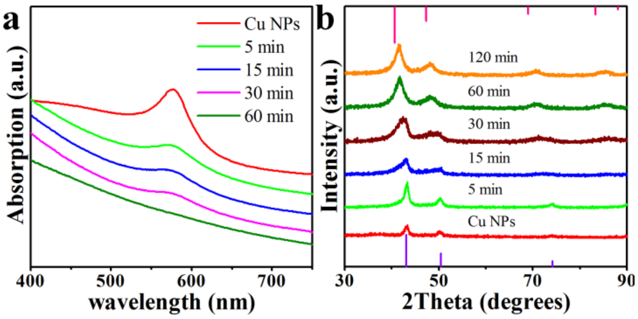

Fig. S5 (a) Absorption spectrum of Cu NPs and temporal absorption spectra with the growth of $Cu_{1.11}Ir$ NCs from 5 to 120 min after the injection of $IrCl_3$-OLA solution into Cu colloidal solution at 250 ^{o}C; (b) XRD pattern of Cu NPs and temporal XRD patterns with the growth of $Cu_{1.11}Ir$ NCs from 5 to 120 min after the injection of $IrCl_3$-OLA solution into the Cu colloidal solution at 250 ^{o}C.

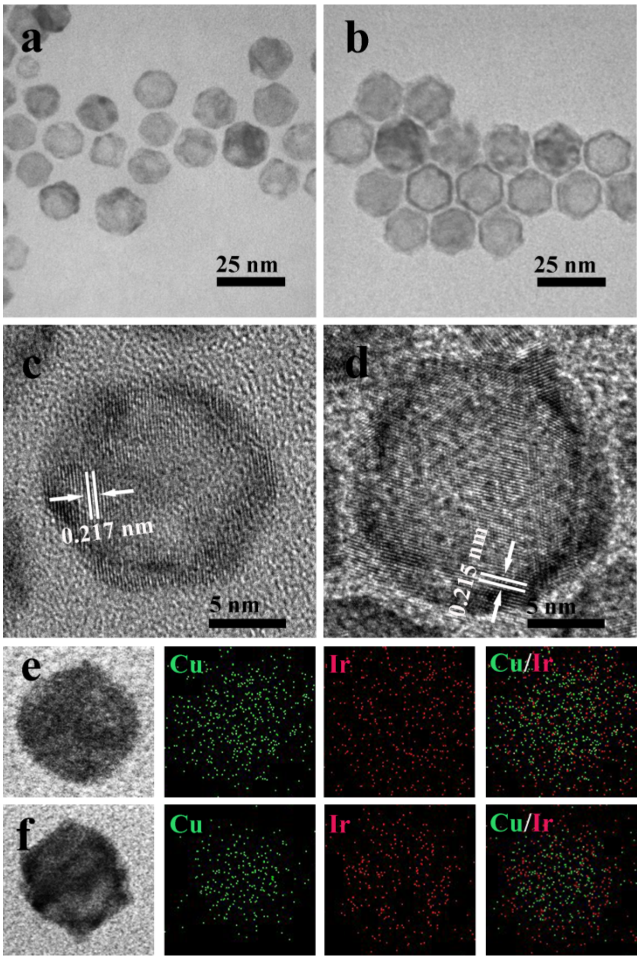

Fig. S6 (a) TEM image, (c) HRTEM image and (e) STEM image and elemental mapping of Cu core Cu-Ir alloy shell nanoparticles obtained with the precursor molar ratio of Ir to Cu of 1:3 with otherwise identical conditions; (b) TEM image, (d) HRTEM image, (f) STEM image and elemental mapping of Cu core Cu-Ir shell nanoparticles obtained with the precursor molar ratio of Ir to Cu of 2:3 with otherwise identical conditions.

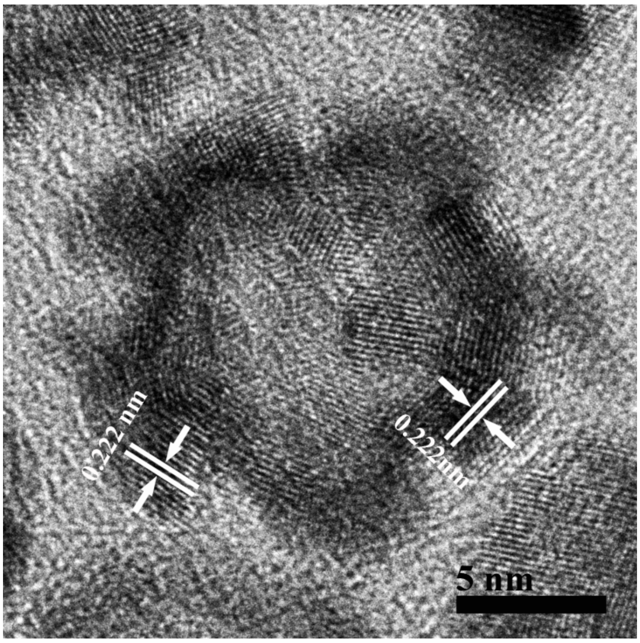

Fig. S7 HRTEM image of a nanocage with Ir branches on their surfaces obtained with the precursor molar ratio of Ir to Cu of 5 : 4.

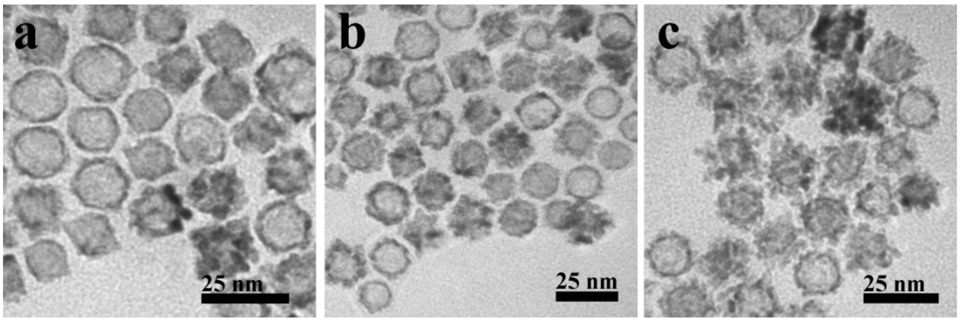

Fig. S8 TEM images of the as-prepared Cu-Ir nanoparticles $Cu_{0.95}Ir$ (a), $Cu_{0.86}Ir$ (b) and $Cu_{0.66}Ir$ (c), respectively.

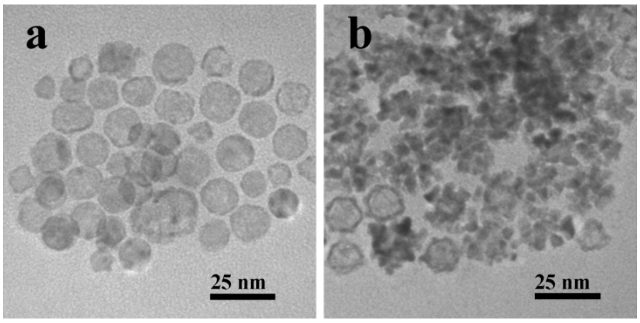

Fig. S9 (a) TEM images of the as-prepared products obtained at 230 ^{o}C with otherwise identical conditions; (b) TEM images of the as-prepared products obtained at 270 ^{o}C with otherwise identical conditions.

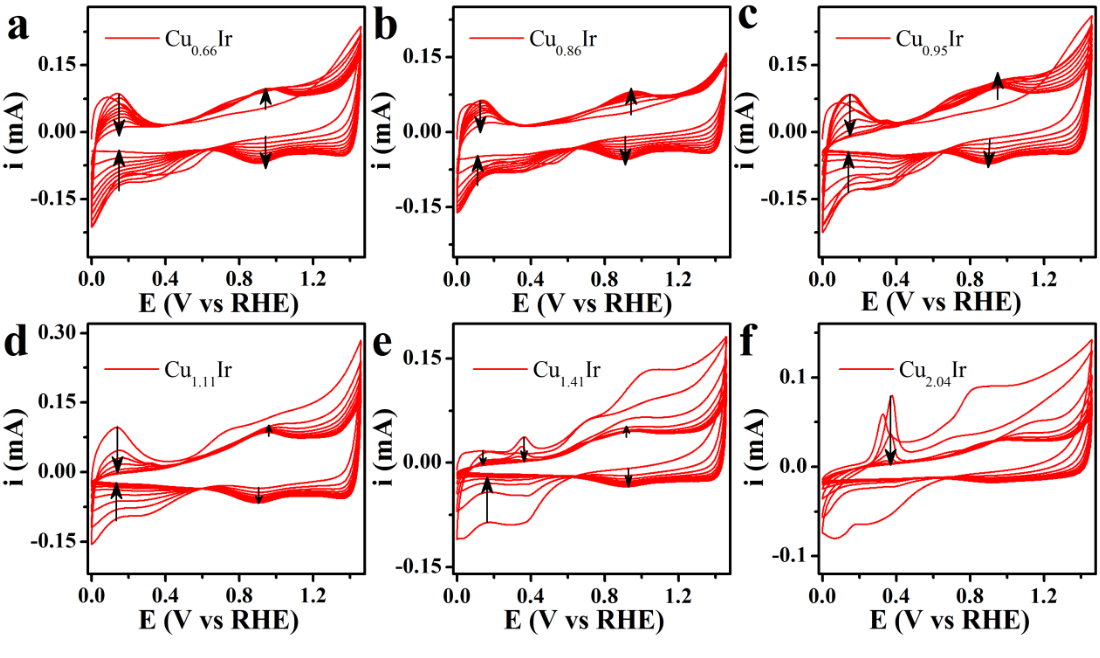

Fig. S10 Voltammetric surface oxidation $Cu_{0.66}Ir$ (a), $Cu_{0.86}Ir$ (b), $Cu_{0.95}Ir$ (c), $Cu_{1.11}Ir$ (d), $Cu_{1.41}Ir$ (e), $Cu_{2.04}Ir$ (f).

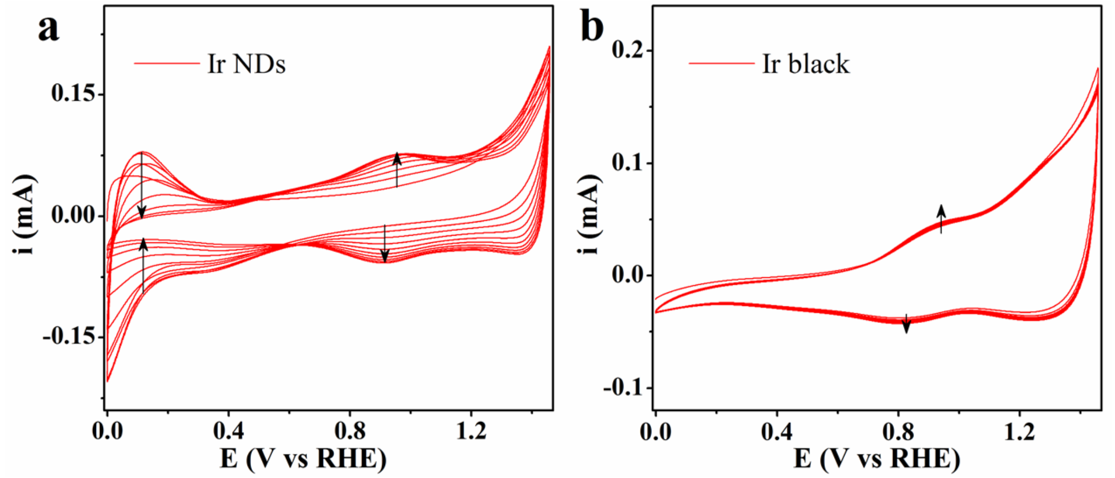

Fig. S11 Voltammetric surface oxidation Ir NDs (a) and Ir black (b).

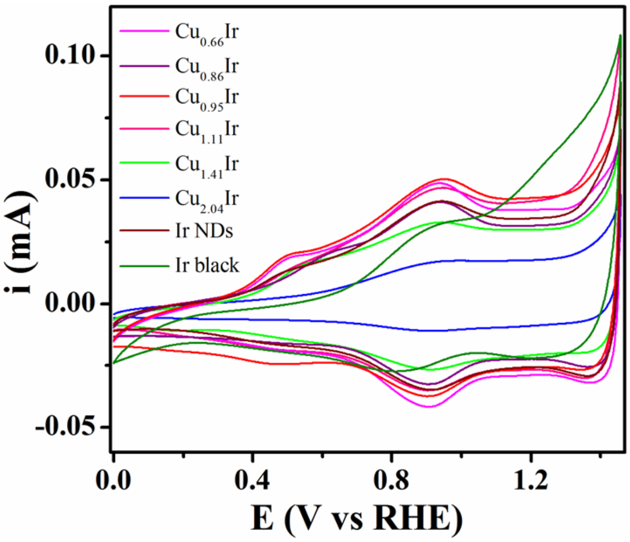

Fig. S12 Ir (III-IV) redox peaks of Cu$_{0.66}$Ir, Cu$_{0.86}$Ir, Cu$_{0.95}$Ir, Cu$_{1.11}$Ir, Cu$_{1.41}$Ir, Cu$_{2.04}$Ir, Ir NDs and Ir black.

Table S1. Evaluated amount of active Ir sites of all the investigated catalysts in this study.

	Cu$_{0.66}$Ir	Cu$_{0.86}$Ir	Cu$_{0.95}$Ir	Cu$_{1.1}$Ir	Cu$_{1.41}$Ir	Cu$_{2.04}$Ir	Ir NDs	Ir black
(nmol)	0.802	0.835	0.848	0.852	0.563	0.102	0.831	0.390

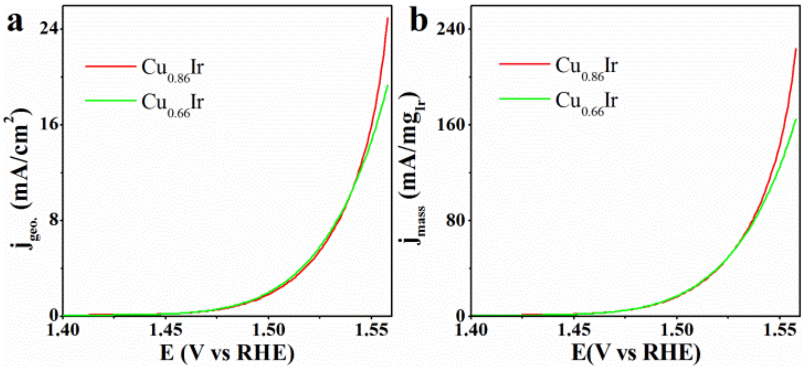

Fig. S13 The polarization curves for OER normalized by the Glass Carbon electrode geometric area (a) and normalized by Ir-based mass (b) at various applied potentials. All measurements were performed in N_2 saturated 0.05 M H_2SO_4 solution at the scan rate of 5 mV/s. All the polarization curves were collected with iR-correction.

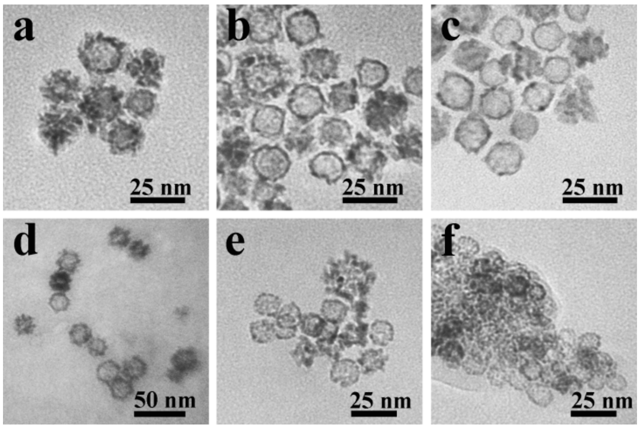

Fig. S14 (a-f) TEM images of $Cu_{0.66}Ir$, $Cu_{0.86}Ir$, $Cu_{0.95}Ir$, $Cu_{1.11}Ir$, $Cu_{1.41}Ir$ and $Cu_{2.04}Ir$, after the electrocatalytic activity and stability tests.

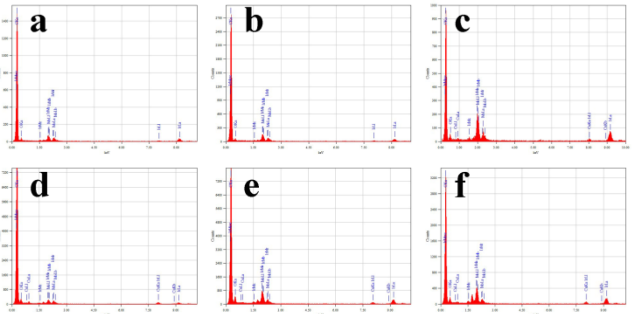

Fig. S15 (a-f) EDX spectra of $Cu_{0.66}Ir$, $Cu_{0.86}Ir$, $Cu_{0.95}Ir$, $Cu_{1.11}Ir$, $Cu_{1.41}Ir$ and $Cu_{2.04}Ir$, after the electrocatalytic activity and stability tests.

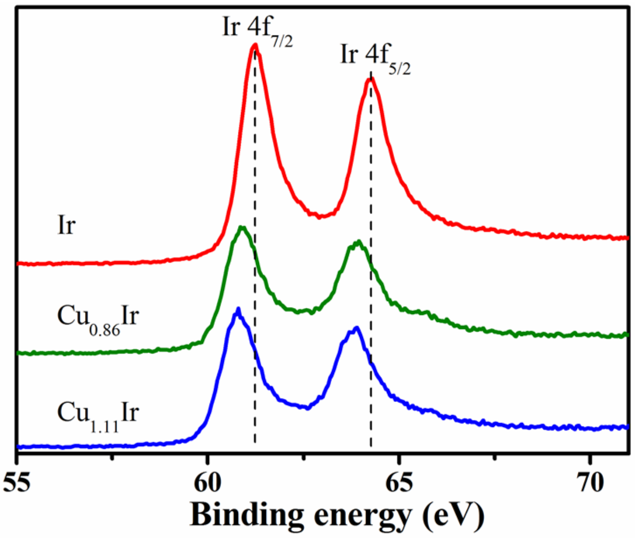

Fig. S16 X-ray photoelectron spectroscopy of Ir, $Cu_{0.86}Ir$ and $Cu_{1.11}Ir$.

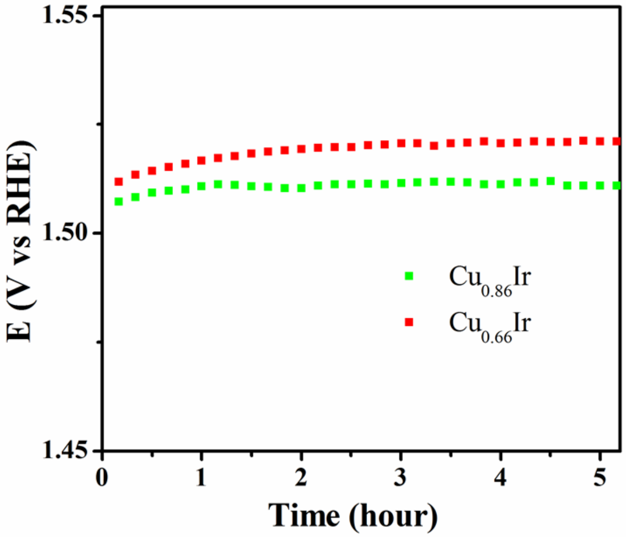

Fig. S17 Chronopotentiometric stability measurements of $Cu_{0.86}Ir$ and $Cu_{0.66}Ir$ at a constant current density of 1 mA/cm^2.

Reference:

[1] C. Wang, G. Xiao, Y. Sui, X. Yang, G. Liu, M. Jia, W. Han, B. Liu, B. Zou, Nanoscale 2014, 6, 15059.